Modeling the Swirling Flow of a Hydrocyclone

B. Chinè[1*], F. Concha [2], M. Meneses G.[3]
1. School of Materials Science and Engineering, Costa Rica Institute of Technology, Cartago, Costa Rica
2. Water Research Center for Agriculture and Mining, CRHIAM, University of Concepción, Chile
3. School of Industrial Production Engineering, Costa Rica Institute of Technology, Cartago, Costa Rica
*Corresponding author: P.O. Box 159-7050, Cartago, Costa Rica, bchine@itcr.ac.cr

Abstract:
Hydrocyclones are industrial devices used as processing units in fluid and particle technology. In a hydrocyclone the fluid and the transported particles experiment high centrifugal forces which force them to move outwards towards the solid walls and then to the bottom exit. On the other hand, the fluid and the particles suffer also an inwardly acting drag which can drive them towards the upper outlet. Thus, the performance of a hydrocyclone depends on the 3D character of this flow and the anisotropy of its turbulence. In this work we have developed a 3D model of the swirling flow in a hydrocyclone by using COMSOL Multiphysics®. Turbulence is modeled by using the Reynolds-Averaged Navier-Stokes equations and the v2-f turbulence closure. The results of the simulations are satisfactory, being able to reproduce the general flow pattern. Finally, the computed velocity profiles are compared with laser Doppler measurements, in order to assess its goodness.

Keywords: hydrocyclone, swirling flow, turbulence, CFD.

1. Introduction

Hydrocyclones [1,2] are industrial devices used as processing units in fluid and particle technology. A hydrocyclone is an apparatus consisting of a cylindrical or a cylindrical-conical body with a tangential or involute entrance to admit the fluid inside (Fig. 1). There are also two opposite exits, the top exit that is the vortex finder and the bottom exit called apex or spigot. In a hydrocyclone, the fluid and the transported particles experiment high centrifugal forces which force them to move outward towards the solid walls and then to flow downwards to the bottom exit. Simultaneously, the fluid and the particles suffer also an inwardly acting drag, which can drive them towards the central region of the vessel. Therefore, fluid and particles travel

Figure 1. A hydrocyclone with tangential inlet.

upwards leaving the vessel through the vortex finder. Furthermore, when the device is open to the atmosphere an air core forms along the hydrocyclone axis. These phenomena and then the performance of the device depend on the complex fluid dynamics developing inside the vessel. The flow pattern results from a three dimensional turbulent swirling flow confined in the cylindrical and conical geometry of the hydrocyclone. A tangential movement, named Rankine vortex, combination of a forced vortex and a free vortex, characterizes this flow. The vortex flow is completed by an axial flow in two opposite directions, one close to the walls towards the apex (underflow discharge) and a reverse flow travelling to the vortex finder, near the center of the hydrocyclone (overflow discharge) [1,2,3,4,5]. The radial component of velocity, playing an important role in the hydrocyclone operation, is one order of magnitude smaller than the other two components, as shown by experimental and theoretical studies.

The 3D character of the flow and the anisotropy of its turbulence [6,7] make difficult and computationally intensive the simulation of the flow in hydrocyclones. Nevertheless, many authors (among others [8,9,10,11]) have applied the Reynolds Averaged Navier-Stokes (RANS)

equations and different anisotropy closures to satisfactorily solve the turbulent flow of the hydrocyclone. In the past Chiné *et al.* [12] applied the finite difference method to obtain a numerical solution for the flow of a two-dimensional hydrocyclone, using the non-isotropic turbulence model of Hsieh and Rajamani [4] based on the Prandtl mixing length hypothesis. The computational results of the velocity, both the axial component and the tangential component, compared well with the experimental values of Hsieh and Rajamani and in particular the Rankine vortex was reproduced. Later, the same authors [13] used Comsol Multiphysics® and the RANS equations with the *k-ω* turbulence model to describe the flow of two-dimensional conical and flat-bottom hydrocyclones. They compared the computational results of the velocity with laser Doppler measurements and demonstrated that, although the general flow pattern was well simulated, the Rankine velocity profile was poorly represented.

In this work, we develop a 3D model of the swirling flow in a conical hydrocyclone by using the CFD module of COMSOL Multiphysics®. Turbulence is modeled by using the Reynolds-Averaged Navier-Stokes equations and the v2-f turbulence closure. The computed velocity profiles are compared with laser Doppler measurements in order to assess its goodness.

The structure of the paper is the following. The description of the physical model and the governing equations are given in Section 2, while Section 3 deals with the use of Comsol Multiphysics®. Finally, the computational results are presented in Section 4 and the conclusions in Section 5.

2. Physical model and governing equations

Fig. 2 shows a schematic and the main geometrical dimensions of the hydrocyclone used in the present study. The diameter *D* of the device is 102 mm, its inlet has a rectangular section with height of 43 mm and width of 16 mm and the diameters of apex and vortex finder are 18 mm and 32 mm, respectively. The hydrocyclone is fed with water and we assume for the modeling work the same values of some experiments carried out in laboratory and given in Table 1. We consider a turbulent, incompressible and single phase flow of a Newtonian fluid. Therefore, the air core is not computed and is represented as a conical solid

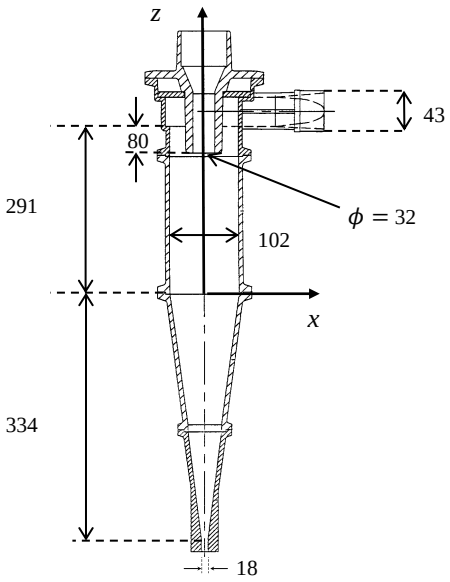

Figure 2. Geometry and main dimensions (in mm) of the hydrocyclone.

Table 1. Experimental values used in the numerical simulations for the water flow of the hydrocyclone.

Magnitude	*Value*
Inlet flowrate *Q*	2.50 l/s
Inlet area *A*= 43 mm x 16 mm	0.688×10^{-3} m^2
Inlet velocity V_{in}	3.63 m/s
Pressure drop Δp	62.05 kPa
Water dynamic viscosity μ	10^{-3} Pa·s
Water density ρ	10^3 kg/m^3
Diameter *D* of the hydrocyclone	102 mm
Mean axial velocity inside the hydrocyclone $V=4Q/\pi D^2$	0.306 m/s
Reynolds number $Re= \rho VD/\mu$	3.12×10^4

tube with estimated diameters from laser Doppler velocimetry measurements [14].

The governing equations are represented by the Navier-Stokes equations, that in vector form and for a time dependent flow read:

$$\frac{\partial \rho}{\partial t} + \nabla \cdot (\rho \boldsymbol{u}) = 0 \qquad (1)$$

$$\rho \frac{\partial \boldsymbol{u}}{\partial t} + \rho(\boldsymbol{u} \cdot \nabla \boldsymbol{u}) = \nabla \cdot (-p\,\mathbf{I} + \boldsymbol{\tau}) + \mathbf{F} \qquad (2)$$

Eq. 1 yields the mass conservation and Eq. 2 describes the linear momentum conservation, where ρ is the density of the fluid, $\boldsymbol{u}$ is the velocity field, p is the pressure, $\mathbf{I}$ is the identity tensor, $\mathbf{F}$ is the body force vector, $\boldsymbol{\tau} = \frac{1}{2}\,\mu\,(\boldsymbol{\nabla u} + (\boldsymbol{\nabla u})^T)$ is the viscous stress tensor and μ is the dynamic viscosity. Then, for a steady state,

incompressible turbulent flow, decomposition of the flow field into an averaged part and a fluctuating one, followed by insertion into Eq. 1 and Eq. 2, gives the Reynolds-Averaged Navier-Stokes (RANS) equations [15,16]:

$$\rho \nabla \cdot \mathbf{U} = 0 \tag{3}$$

$$\rho \frac{\partial \mathbf{U}}{\partial t} + \rho \mathbf{U} \cdot \nabla \mathbf{U} + \nabla \cdot (\overline{\rho \boldsymbol{u}' \boldsymbol{u}'}) = -\nabla \mathrm{P} + \nabla \cdot \mu(\nabla \mathbf{U} + (\nabla \mathbf{U})^{T}) + \mathbf{F} \tag{4}$$

where $\mathbf{U}$ is the averaged velocity field and $\overline{\rho \boldsymbol{u}' \boldsymbol{u}'}$ is the Reynolds stress tensor. The term $\overline{\rho \boldsymbol{u}' \boldsymbol{u}'}$, which must be modeled in order to close Eq. 4, can be computed by using the Boussinesq hypothesis and relating this stress to mean velocity gradients and turbulent viscosity.

3. Solution with Comsol Multiphysics®

The strong anisotropy of the flow lead us to discard isotropic turbulence description in favour of the v2-f turbulence model. This model assumes that the turbulent viscosity is based on the velocity fluctuations $\overline{v^2}$ normal to the streamlines, making it possible to represent turbulence anisotropy [15]. The v2-f turbulence model may be reviewed in the work of Billiard [16] and its equations are also given in [15].

Using Comsol Multiphysics® 5.3a we study the swirling flow of the hydrocyclone by using the CFD Module and the Turbulent Flow v2-f physical interface with default parameters. The geometry of the vessel is created in the same software, by revolving a plane section of the hydrocyclone into a 3D space and with a successive union of the inlet tube. Next, boundary conditions are specified in order to solve the resulting system of partial differential equations. In particular, we set a velocity V_{in} of 3.63 m/s on the inlet and the condition of zero normal stress on both outlets. Furthermore, we use the no slip condition on the solid walls of the hydrocyclone and the slip condition on the artificial surface of the conical air core. The values of turbulence intensity and turbulence length scale are 0.05 and $0.07D_{eq}$ respectively, where D_{eq} is the diameter of an equivalent circular inlet section A of area equal to $43x16$ mm^2. The initial values of the computed magnitudes are the default values set by the software. The unstructured meshing of the computational region is accomplished by dividing it with free tetrahedral volumes and applying *fine* (size 1) element in the hydrocyclone domain and *finer* (size 2) element on the solid walls. The element size parameters are given in Table 2. Additionally, nine boundary layers are generated on the same solid walls, using default values of the software. Then, the numerical computations are carried out by developing a first study (*Wall Distance Initialization*) to calculate the reciprocal wall distance of the v2-f turbulence model and a stationary second study to compute the swirling turbulent flow of the hydrocyclone. The number of degrees of freedom to be solved for is approximately $1.2x10^5$ for the wall distance initialization step and nearly $9.5x10^5$ for the subsequent stationary step.

Table 2. Size of mesh elements.

Parameter	*Size*
Maximum element of size 1	6 mm
Minimum element of size 1	0.4 mm
Maximum element of size 2	6 mm
Minimum element of size 2	0.2 mm

4. Results and discussion

Fig. 3 plots the streamlines of the swirling flow inside the hydrocyclone, indicating the presence of a forward fluid motion close to the solid walls of the device and a reverse fluid motion around the vertical longitudinal axis. According to the computational simulations, the reverse flow starts at 25% of the hydrocyclone height, approximately. This is confirmed by the

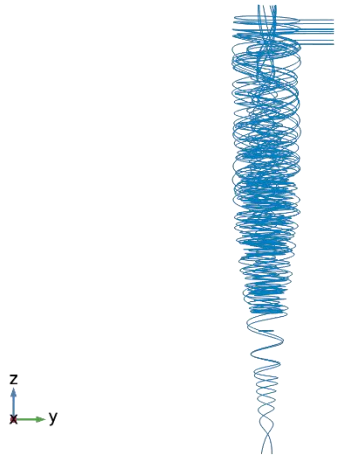

Figure 3. Computed streamlines of the swirling flow in the hydrocyclone.

axial velocity profile at z = -180 mm (Fig. 4), showing that the axial velocity is always negative from the centre of the vessel to the walls. The corresponding tangential (swirl) velocity computed at z= -180 mm is shown in Fig. 5, revealing that this component increases with the distance from the surface of the fictitious air core. Conversely, Fig. 6 and Fig. 7 give the velocity profiles at z = +200 mm, representing a height below the vortex finder entrance, placed at z= +211 mm. The axial component of velocity of Fig. 6 depicts a correct flow profile, because the high centrifugal forces force the fluid to move outward towards the solid walls, and then to flow downwards to the bottom exit. Simultaneously, the fluid suffers also an inwardly motion which drive it towards the central region of the vessel and later into the vortex finder. The swirling velocity of Fig. 7 underlines a forced vortex regime close to the air core, followed by an

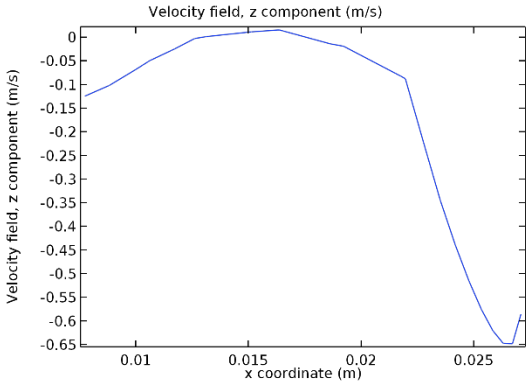

Figure 4. Profile of the axial component of velocity in the hydrocyclone at z = -180 mm.

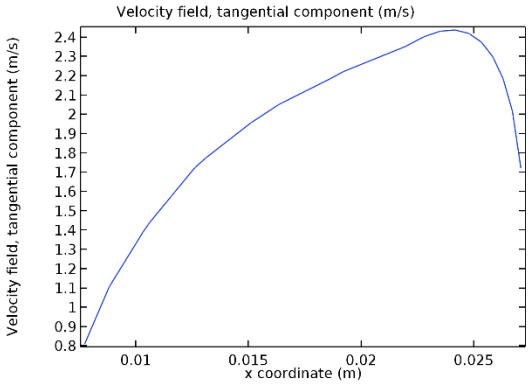

Figure 5. Profile of the tangential component of velocity in the hydrocyclone at z = -180 mm.

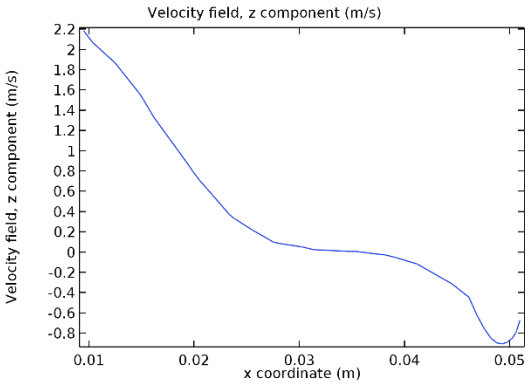

Figure 6. Profile of the axial component of velocity in the hydrocyclone at z = +200 mm.

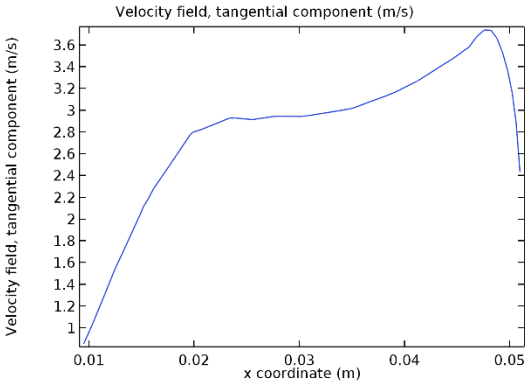

Figure 7. Profile of the tangential component of velocity in the hydrocyclone at z = +200 mm.

external area where the tangential velocity changes its behaviour, although it is different from a free vortex. The integration of the axial component of velocity on both outlets gives the two flowrates Q_u and Q_o, the flowrate of the underflow and the overflow, respectively. The values computed by the numerical simulations are Q_u = 0.4833 l/s and Q_o= 1.9754 l/s, whose sum 2.4587 l/s compares very well with the inlet flowrate Q of 2.5 l/s, with a relative error of 1.65%. The computational results show the effectiveness of boundary conditions and air core sizes specified on the outlets.

Next, we compare the computational results with velocity measurements obtained by laser Doppler velocimetry (LDV), for the same experimental conditions of Table 1. We verify that the axial flow is very well reproduced, while the swirl flows deviates, as demonstrate Fig. 8 and

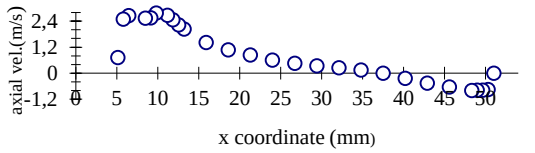

Figure 8. Experimental values by LDV of the axial component of velocity in the hydrocyclone at z = +186 mm.

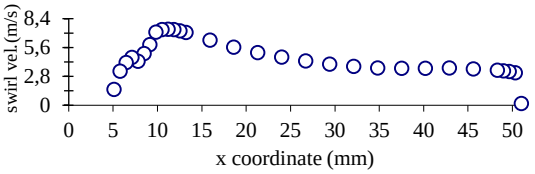

Figure 9. Experimental values by LDV of the tangential component of velocity in the hydrocyclone at z = +186 mm.

Fig. 9, plotting at z= +186 mm the axial and the tangential velocity, respectively. The values of the axial velocity of Fig. 8 well superpose those of Fig. 6, which have been computed, practically for the same z coordinate. Both profiles have the same *locus* of zero axial velocity and very coincident upward maximum (2.2 m/s) and downward maximum (0.9 m/s) values of this component. On the contrary, the Rankine vortex of Fig. 9 measured by the LDV technique is not reproduced in Fig. 7, even though this graph shows a sharp change of the tangential velocity. The computational results of Fig. 7 reveal that the rigid body rotation of the central region modifies correctly to a different rotation pattern, when moving towards external regions, but the free vortex flow is not well simulated.

Therefore, by considering v2-f model able to model turbulence anisotropy, starting from these results we conclude that the computational model might be improved. In this case, mesh sizes may represent a limitation since computational capabilities and computing times must be taken into account for.

5. Conclusions

In this work we have developed a 3D model of the swirling flow in a conical hydrocyclone by using the CFD module of COMSOL Multiphysics®. The turbulence of the flow has been modeled by using the Reynolds-Averaged Navier-Stokes equations and the v-2f turbulence closure. The results of the simulations are satisfactory, being able to reproduce the general pattern of this complex flow. Finally, the computed velocity profiles have been compared with laser Doppler measurements, in order to assess its goodness.

6. References

[1] D. Bradley, *The hydrocyclone*, Pergamon, London (1965).
[2] L. Svarovsky, *Hydrocyclones*, Holt, Rinehart and Winston, London, 1984.
[3] D.F. Kelsall , A study of the motion of solid particles in a hydraulic cyclone, *Trans. Instn Chem. Engrs*, **30** , 87-108 (1952).
[4] K.T. Hsieh and R.K. Rajamani , Mathematical model of the hydrocyclone based on physics of fluid flow, *AIChE Journal* **37**(5), 735-746 (1991).
[5] F. Concha, Flow pattern in hydrocyclones, *KONA Powder and Particle Journal*, **25**, 97-132 (2007).
[6] F. Boysan, W.H. Ayers and J. Swithenbank, A fundamental mathematical modelling approach to cyclone design, *Trans. Instn. Chem. Engrs.*, **60**, 221-230 (1982).
[7] A.F. Nowakoswksi and M. J. Doby, The numerical modelling of the flow in hydrocyclones, *KONA Powder and Particle Journal*, **28**, 66-80 (2008).
[8] A. Davailles, E. Climent and F. Bourgeois, Fundamental understanding of swirling flow pattern in hydrocyclones, *Separation and Purification Technology*, **92**, 152-160 (2012).
[9] Y. Rama Murthy and K. Udaya Bhaskar, Parametric CFD studies on hydrocyclone, *Powder Technology*, **230,** 36-47 (2012).
[10] T.R. Vakamalla and N. Mangadoddy, Numerical simulation of industrial hydrocyclones performance: Role of turbulence modelling, *Separation and Purification Technology*, 176, 23-39 (2017).
[11] D. Pérez, P. Cornejo, C. Rodríguez and F. Concha, Transition from spray to roping in hydrocyclones, *Minerals Engineering*, **123**, 71-84 (2018).
[12] B. Chiné, F. Concha and A. Barrientos, A finite difference solution of the swirling flow in a hydrocyclone, *Proceed. of the Inter. Conf. on Finite Elements in Fluids-New trends and applications*, Venezia, Italy, 15-21 October (1995).

[13] B. Chiné, F. Concha and M. Meneses G., A 2D Model of the flow in hydrocyclones, *Comsol Conference 2014*, Cambridge, England, 17-19 September (2014).
[14] B. Chiné and F. Concha, Flow patterns in conical and cylindrical hydrocyclones, *Chemical Engineering Journal*, **80**(1-3), 267-274 (2000).
[15] Comsol AB, Comsol Multiphysics-CFD Module, *User's Guide*, Version 5.3a (2017).
[16] F. Billiard, Near-wall turbulence RANS modeling and its applications to industrial cases, *MPhil Thesis*, University of Manchester, England, (2007).

7. Acknowledgements

The authors gratefully acknowledge the University of Concepción and the financial aid provided by the Vicerrectoria de Investigaciòn y Extensiòn of the Instituto Tecnològico de Costa Rica.